Wood Sci Technol (2014) 48:51–58
DOI 10.1007/s00226-013-0570-7

ORIGINAL

Preliminary observations of hydrothermal growth of nanomaterials on wood surfaces

Qingfeng Sun · Yun Lu · Dongjiang Yang · Jian Li · Yixing Liu

Received: 8 January 2012 / Published online: 3 July 2013

Abstract A hydrothermal method of fabricating nanomaterials at wood surfaces is described in this paper. Nanomaterials with different morphologies including spherical anatase TiO_2, amorphous SiO_2, wurtzite ZnO nanorod arrays, intertwining MnO_2 nanowires, shuttle-shaped $CaCO_3$ nanorods, and rhombic and cubic NaCl were deposited at wood surfaces. TiO_2–ZnO compound nanoparticles and CuO nanoparticles were also created. The surface morphologies and crystalline structures of the prepared samples were characterized by scanning electron microscopy and X-ray diffraction, respectively. No obvious changes in the color of wood were caused by the hydrothermal process except those nanomaterials of Mn or Cu deposited at surfaces.

Introduction

Wood continues to be used for a lot of applications because of its many excellent material properties, such as a good strength to weight ratio, esthetic appearance, etc., but it also suffers from a number of disadvantages. Dimensional changes in

Qingfeng Sun and Yun Lu are co-first authors.

Q. Sun (✉) · Y. Lu · J. Li · Y. Liu
Key Laboratory of Bio-based Material Science and Technology, Ministry of Education, Northeast Forestry University, No. 26 Hexing Road, Xiangfang District, Harbin 150040, People's Republic of China
e-mail: qfsun@nefu.edu.cn

Y. Liu
e-mail: yxliu@nefu.edu.cn

D. Yang
College of Chemistry, Chemical and Environmental Engineering, Qingdao University, Qingdao 266071, People's Republic of China

response to changing atmospheric conditions, susceptibility to fire, and biological attack and changes in appearance when exposed to weathering place restrictions on the potential end-uses of wood (LeVan and Winandy 1990; Kumar 1994; Hill 2006; Kataoka et al. 2007). Bulk modification can be problematic due to the difficulty of ensuring evenly dispersion of the reagents throughout the wood material and that all excess reagents and by-products are removed at the end of the reaction (Collett 1972; Kumar 1994; Sèbe and Brook 2001; Mai and Militz 2004; Hansmann et al. 2005; Rautkari et al. 2009). However, if the reaction is confined to the surface of the wood substrates, then accessibility of reagent and subsequent cleanup of the modified material are more easily accomplished. Surface modification of wood has been used to improve the ultraviolet stability of wood, to change the surface energy of wood (to reduce wetting by water and/or improve compatibility with coatings or matrix materials), and to improve bonding between wood surfaces (Subramaniana et al. 1982; Williams 1983; Ghosh 2006; Bourbigot and Duquesne 2007; Marney and Russell 2008; Jebrane et al. 2009; Sun et al. 2010a). The currently widely used methods for surface modification are summarized as coating, grafting, sol–gel methods, plasma, or corona discharge, etc. (Kumar 1994; Miyafuji and Saka 2001; Tshabalala and Sung 2007; Hill 2006; Zanini et al. 2008; Evans and Chowdhury 2010; Jamali and Evans 2011; Wang and Piao 2011). There is also interest in developing other methods for surface modification of wood. One such method is hydrothermal modification.

Hydrothermal process is normally conducted in Teflon-lined steel pressure vessels under controlled temperature and/or pressure with the reaction occurring in solution (Byrappa and Adschiri 2007; Yang et al. 2008, 2009, 2011). The temperature can be elevated above the boiling point of water or other solutions, reaching the pressure of vapor saturation. The temperature and the amount of solution added to the autoclave largely determine the internal pressure produced. It is a promising method that is widely used for the synthesis of different kinds of nanomaterials. It has not been widely used for wood surface modification. However, a previous research has confirmed that hydrothermal method is a facile method for the growth of TiO_2 structures (Li et al. 2010; Sun et al. 2010a, b, 2011). Hence, the hydrothermal method appeared to be a promising method for wood surface modification. Herein, the deposition of eight different kinds of nanomaterials at wood surfaces is described. The results of this study demonstrate that the hydrothermal method is a facile and useful method for wood surface modification.

Materials and methods

Materials

All the chemicals were supplied by Shanghai Boyle chemical Co. Ltd. Wood specimens from air-dried poplar lumber were cut into a size of 20 mm (longitudinal) × 20 mm (tangential) × 10 mm (radial). The volume of autoclave is general 100 mL. The generated pressure is common from 0.3 to 3 MPa. The temperature can be set. The lining is Teflon.

Hydrothermal growth of nanomaterials on wood surface

The common hydrothermal process is described as follows: When the required solutions are prepared, wood samples were dipped into the solutions and transferred into a Teflon-lined stainless steel autoclave. After each treatment, the specimens were removed from the solution, ultrasonically rinsed with deionized water for 30 min, and dried at 45 °C for over 24 h in vacuum.

TiO_2/wood

1 mL of tetrabutyl orthotita (TBOT) was first dissolved in 40 mL of anhydrous ethyl alcohol with magnetic stirring for 30 min at room temperature. The autoclave was sealed and maintained at 130 °C for 4 h and then cooled to room temperature naturally. After this heating process, the autoclave was opened, and 40 mL 9.1×10^{-4} mol/L sodium dodecyl sulfate solution at a pH of 6.5 was added. The autoclave was then sealed again and maintained at 70 °C for 4 h and then cooled to room temperature naturally.

SiO_2/wood

A mixture of ethanol (42.5 mL), H_2O (4.5 mL), and NH_4OH (0.75 mL), under moderate stirring followed by addition of tetraethoxysilane (TEOS, 2.25 mL), was transferred into a Teflon-lined stainless steel autoclave. Wood specimens were subsequently placed into the above reaction solution. The autoclave was sealed and maintained at 120 °C for 18 h and then cooled to room temperature naturally.

ZnO nanorod arrays/wood

(1) Fifty-two milliliter of 0.01 M alcoholic zinc acetate solution was heated to 60 °C under vigorous stirring. Then, 26 mL of 0.03 M alcoholic sodium hydroxide was dropwise added and stirred for 2 h at 60 °C. Thus, a transparent and stable ZnO colloid was obtained. The as-prepared ZnO colloid was coated onto the wood surface by a dip-coating process. Wood specimens were immersed into the ZnO colloid for 5 min. After that, the modified samples were dried at 105 °C for 3 h. This process was repeated for 8–10 times. The prepared samples were collected for further hydrothermal treatment. (2) An equimolar (0.015 M) aqueous solution of zinc nitrate hexahydrate and hexamethylenetetramine was gathered as the reacting solution. For hydrothermal growth of ZnO nanorod arrays, 40 mL of each solution was mixed together and transferred into a Teflon-lined stainless steel autoclave. Wood specimens coated by ZnO nanoseeds were subsequently placed into the above reaction solution. The autoclave was sealed and maintained at 95 °C for 8 h and then cooled to room temperature naturally.

MnO_2/wood

2 mmol $KMnO_4$ and 2 mmol NH_4F were dissolved in 80 mL deionized water to form a clear solution under magnetic stirring. The autoclave was sealed and maintained at 150 °C for 18 h and then cooled to room temperature naturally.

TiO_2–ZnO/wood

0.7 g of tetrabutyl orthotita, 0.36 g of zinc nitrate hexahydrate, and 0.168 g of hexamethylenetetramine were added to 80 mL absolute ethanol in a capped bottle. The solution was stirred for 3–5 h to generate a homogeneous solution. Then, the solution was transferred into a 100 mL autoclave. Wood specimens were subsequently placed into the above reaction solution. The autoclave was sealed and maintained at 110 °C for 18 h and then cooled to room temperature naturally. Finally, the prepared samples were removed from the solution, ultrasonically rinsed with deionized water for 30 min, and dried at 45 °C for over 24 h in vacuum.

CuO/wood

80 mL of aqueous solution containing 0.5 M copper acetate and 0.5 M urea was transferred into a Teflon-lined autoclave of 100 mL capacity. The autoclave was sealed and maintained at 120 °C for 2 h and then cooled to room temperature naturally.

$CaCO_3$/wood

0.01 M of calcium acetate and 0.02 M of urea were dissolved in 80 mL deionized water to form a clear solution under vigorously magnetic stirring. The autoclave was sealed and maintained at 120 °C for 4 h and then cooled to room temperature naturally. After reaction, 2 mL oleic acid and 0.2 g polyacrylamide were added and maintained at 80 °C for 20 h.

NaCl/wood

0.005 M sodium chloride was dissolved in 40 mL deionized water under magnetic stirring. The autoclave was sealed and maintained at 120 °C for 18 h and then cooled to room temperature naturally. After this heating process, the autoclave was opened, and 40 mL 1×10^{-4} mol/L hexadecyl trimethyl ammonium bromide with pH value of 3 was added. The autoclave was then sealed again and maintained at 120 °C for 4 h and then cooled to room temperature naturally.

Characterization

Surface morphologies of the samples were characterized by environmental scanning electron microscopy (SEM) using a FEI-SEM Quanta 200 microscope operating at 12.5 kV. Samples were sputter coated with gold. Crystalline structures of the samples were identified by X-ray diffraction technique (XRD, Rigaku, D/MAX 2200) operating with Cu K_α radiation ($\lambda = 1.5418$ Å) at a scan rate (2θ) of 4°/min and an accelerating voltage of 40 kV and an applied current of 30 mA ranging from 5° to 70°.

Results and discussion

Figure 1 shows SEM images of wood and different nanomaterials deposited at wood surfaces using the hydrothermal method. In Fig. 1a, unmodified poplar wood surface with intervascular alternate pits can be clearly observed from the SEM image. In Fig. 1b, continuous TiO_2 coating apparently covered the entire surface of the wood remaining intact and smooth. Some TiO_2 spheres approximately 300–600 nm in diameter are evenly dispersed on the thin coating. In Fig. 1c, the hydrothermal hydrolysis of TEOS produced discrete SiO_2 spheres, approximately 100–500 nm in diameter coating the wood surface. This compact coating probably results from the condensation of silica oligomers, which become attached to the wood surface during the hydrothermal growth process (Pinto et al. 2008). In Fig. 1d, it is clear that the ZnO nanorod arrays with a uniform height were densely and evenly attached to the wood surface. The cross-section inset in Fig. 1d indicates that the length of the ZnO nanorod arrays was about 1.5 μm. In Fig. 1e, it is obvious that the wood surface was densely covered by MnO_2 nanowires. The inset image clearly shows that MnO_2 nanowires are cross-linking and intertwining with a length of 10–30 μm and a diameter of 10–80 nm. In Fig. 1f, it is clear that the wood surface was densely covered by TiO_2–ZnO particles. The size of TiO_2–ZnO nanoparticles is 80–200 nm observed from the SEM image. In Fig. 1g, the wood pits and surface are completely covered by CuO nanoparticles. The size of CuO nanoparticles is 50–200 nm. In Fig. 1h, it appears that shuttle-shaped $CaCO_3$ nanorods with a diameter of 80–400 nm and a length of 1–2 μm totally coated the wood surface. Wood features cannot be clearly observed in this SEM image. In Fig. 1i, it can be seen that rhombic and cubic NaCl covered the wood surfaces. The length and width of hydrothermally grown NaCl were 100–1,000 and 80–200 nm, respectively.

X-ray diffractography can determine the crystal structure and lattice parameters of crystalline materials. The JCPDS database can be used for phase identification of unknown samples by comparing diffraction scans with the scan (card) of some specific crystal from the JCPDS database. Figure 2 shows XRD patterns of unmodified wood and different nanomaterials. In Fig. 2a, the diffraction peaks at about 15° and 22° assigned to wood are present (Kalliat et al. 1983; Paakkari and Serimaa 1984; Kumar et al. 1993; Sarén and Serimaa 2006). Figure 2b indicates that

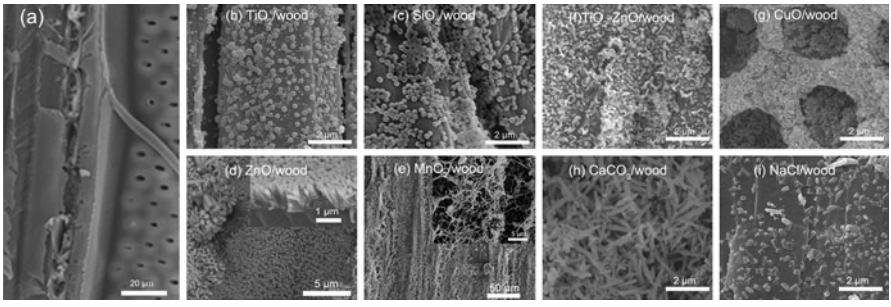

Fig. 1 SEM images of **a** unmodified wood and **b–i** different nanomaterials at wood surfaces (**b** TiO_2, **c** SiO_2, **d** ZnO nanorod arrays, **e** MnO_2, **f** TiO_2–ZnO, **g** CuO, **h** $CaCO_3$, **i** NaCl)

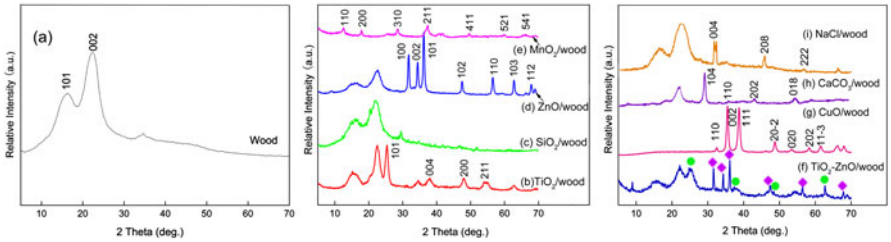

Fig. 2 XRD patterns of **a** unmodified wood and *b*–*i* different nanomaterials at wood surfaces (*b* TiO_2, *c* SiO_2, *d* ZnO nanorod arrays, *e* MnO_2, *f* TiO_2–ZnO, *g* CuO, *h* $CaCO_3$, *i* NaCl). *Diamond* indicates the wurtzite phase of ZnO, and *circle* indicates the anatase phase of TiO_2

Fig. 3 Macroscopic images of **a** unmodified wood and **b**–**i** different nanomaterials/wood (**b** TiO_2, **c** SiO_2, **d** ZnO nanorod arrays, **e** MnO_2, **f** TiO_2–ZnO, **g** CuO, **h** $CaCO_3$, **i** NaCl)

the crystalline phase of wood surfaces treated with TiO_2 was dominated by the characteristic peaks of anatase TiO_2 (JCPDS: 21-1272) and wood. XRD patterns confirm that a film of anatase TiO_2 was presented at wood surfaces. In Fig. 2c, it is clear that the crystalline structure of the sample was not different compared with that of pure wood, which indicates the as-prepared SiO_2 spheres grown on wood surface are amorphous with no crystalline phases. In Fig. 2d, some new strong diffraction peaks are observed in ZnO/wood sample, indicating the formation of new crystal structure at the wood surface. For ZnO/wood sample, all diffraction peaks could be assigned to the wurtzite-type ZnO (JCPDS: 36-1451). No excess peaks were detected, implying that only high purity ZnO nanostructure was formed following the hydrothermal reaction. In Fig. 2e, all the diffraction peaks can be readily assigned to pure body-centered tetragonal α-MnO_2 phase (JCPDS: 44-0141). No diffraction peaks are observed for impurities, suggesting the high purity of the final products. In addition, the diffraction peaks of the pure wood are not present which suggests that a relatively dense MnO_2 film was formed at the wood surface. This can also be confirmed by the macroscopic images (Fig. 3e). The color of MnO_2/wood was brown. In Fig. 2f, new diffraction peaks could be assigned to wurtzite-type ZnO and anatase TiO_2. These observations indicate that the TiO_2–ZnO coating has been successfully deposited at the surface of the wood. In Fig. 2g, all of the diffraction peaks can be clearly assigned to CuO (JCPDS: 48-1548). No

other impurities were detected by XRD analysis, indicating a high purity for the CuO nanoparticles. Additionally, the diffraction peaks of the pure wood are not observed, demonstrating that a relatively dense CuO film was formed at the wood surface. This can also be confirmed by the macroscopic images (Fig. 3g). The CuO/wood was a brownish red color. In Fig. 2h, new strong diffraction peaks are in good agreement with $CaCO_3$ crystal (JCPDS: 47-1743). In Fig. 2i, the new diffraction peaks can be assigned to NaCl crystal (JCPDS: 05-0628). No other peaks were detected, implying that only high purity NaCl nanostructure was formed at the wood surface after the hydrothermal reaction.

Figure 3 shows macroscopic images of the unmodified and modified wood, respectively. The unmodified wood appears pale yellow. There was no obvious change in the color of the wood modified with TiO_2 or SiO_2 (Fig. 3b, c). In contrast, the MnO_2/wood appears in saturated dark green color (Fig. 3e). TiO_2–ZnO/wood and $CaCO_3$/wood were a little paler in comparison with the unmodified wood (Fig. 3f, h). CuO/wood was a brownish red (Fig. 3g). The appearance of NaCl/wood (Fig. 3i) was faint yellow possibly due to the alkaline acidic surroundings during the hydrothermal process.

Conclusion

Eight kinds of nanomaterials were successfully deposited at wood surfaces through the hydrothermal method. It is confirmed that the hydrothermal method is a useful route for depositing different nanomaterials at wood surfaces. The morphology of these nanomaterial/wood hybrid materials can be altered according to the parent materials used for the reaction. Further research is required to assess property improvements to wood from the hydrothermal deposition of nanomaterials at wood surface.

Acknowledgments This work was supported by the Breeding Plan of Excellent Doctoral Dissertation of Northeast Forestry University (GRAP09), the Program of Introducing Talents of Discipline to Universities of China (B08016).

References

Bourbigot S, Duquesne S (2007) Fire retardant polymers: recent developments and opportunities. J Mater Chem 17:2283–2300

Byrappa K, Adschiri T (2007) Hydrothermal technology for nanotechnology. Prog Cryst Growth Charact Mater 53:117–166

Collett BM (1972) A review of surface and interfacial adhesion in wood science and related fields. Wood Sci Technol 6:1–42

Evans PD, Chowdhury M (2010) Photoprotection of wood using polyester-type UV-absorbers derived from the reaction of 2-hydroxy-4(2,3-epoxypropoxy)-benzophenone with dicarboxylic acid anhydrides. J Wood Chem Technol 30:186–204

Ghosh SK (2006) Functional coatings and microencapsulation: a general perspective. Wiley-VCH Verlag GmbH & Co. KGaA, Weinheim

Hansmann C, Weichslberger G, Gindl W (2005) A two-step modification treatment of solid wood by bulk modification and surface treatment. Wood Sci Technol 39:502–511

Hill CAS (2006) Wood modification: chemical, thermal and other processes. Wiley, Chichester

Jamali A, Evans PD (2011) Etching of wood surfaces by glow discharge plasma. Wood Sci Technol 45:169–182

Jebrane M, Sèbe G, Cullis I, Evans PD (2009) Photostabilisation of wood using aromatic vinyl esters. Polym Degrad Stab 94:151–157

Kalliat M, Kwak CY, Schmidt PW, Cutter BE, McGinnes EA (1983) Small angle X-ray scattering measurement of porosity in wood following pyrolysis. Wood Sci Technol 17:241–257

Kataoka Y, Kiguchi M, Williams R, Evans PD (2007) Violet light causes photodegradation of wood beyond the zone affected by ultraviolet light. Holzforschung 61:23–27

Kumar S (1994) Chemical modification of wood. Wood Fiber Sci 26(2):270–280

Kumar M, Gupta RC, Sharma T (1993) X-ray diffraction studies of *Acacia* and *Eucalyptus* wood chars. J Mater Sci 28:805–810

LeVan S, Winandy J (1990) Effects of fire retardant treatments on wood strength: a review. Wood Fiber Sci 22:113–131

Li J, Yu H, Sun Q, Liu Y, Cui Y, Lu Y (2010) Growth of TiO_2 coating on wood surface using controlled hydrothermal method at low temperatures. Appl Surf Sci 256(16):5046–5050

Mai C, Militz H (2004) Modification of wood with silicon compounds. Treatment systems based on organic silicon compounds—a review. Wood Sci Technol 37:453–461

Marney DCO, Russell LJ (2008) Combined fire retardant and wood preservative treatments for outdoor wood applications—a review of the literature. Fire Technol 44:1–14

Miyafuji H, Saka S (2001) Na_2O–SiO_2 wood-inorganic composites prepared by the sol-gel process and their fire-resistant properties. J Wood Sci 47:483–489

Paakkari T, Serimaa R (1984) A study of the structure of wood cells by x-ray diffraction. Wood Sci Technol 18:79–85

Pinto RJB, Marques PAAP, Barros-Timmons AM, Trindade T, Neto CP (2008) Novel SiO_2/cellulose nanocomposites obtained by in situ synthesis and via polyelectrolytes assembly. Compos Sci Technol 68:1088–1093

Rautkari L, Properzi M, Pichelin F, Hughes M (2009) Surface modification of wood using friction. Wood Sci Technol 43:291–299

Sarén M-P, Serimaa R (2006) Determination of microfibril angle distribution by X-ray diffraction. Wood Sci Technol 40:445–460

Sèbe G, Brook MA (2001) Hydrophobization of wood surfaces: covalent grafting of silicone polymers. Wood Sci Technol 35:269–282

Subramaniana RV, Balabaa WM, Somasekharan KN (1982) Surface modification of wood using nitric acid. J Adhes 14(3–4):295–304

Sun Q, Yu H, Liu Y, Li J, Cui Y, Lu Y (2010a) Prolonging the combustion duration of wood by TiO_2 coating synthesized using cosolvent-controlled hydrothermal method. J Mater Sci 45:6661–6667

Sun Q, Yu H, Liu Y, Li J, Lu Y, Hunt JF (2010b) Improvement of water resistance and dimensional stability of wood through titanium dioxide coating. Holzforschung 64:757–761

Sun Q, Lu Y, Liu Y (2011) Growth of hydrophobic TiO_2 on wood surface using a hydrothermal method. J Mater Sci 46:7706–7712

Tshabalala M, Sung L-P (2007) Wood surface modification by in situ sol–gel deposition of hybrid inorganic–organic thin films. J Coat Technol Res 4:483–490

Wang C, Piao C (2011) From hydrophilicity to hydrophobicity: a critical review—part II: hydrophobic conversion. Wood Fiber Sci 43:41–56

Williams RS (1983) Effect of grafted UV stabilizers on wood surface erosion and clear coating performance. J Appl Poly Sci 28(6):2093–2103

Yang D, Zheng Z, Zhu H, Liu H, Gao X (2008) Titanate nanofibers as intelligent absorbents for the removal of radioactive ions from water. Adv Mater 20:2777–2781

Yang D, Liu H, Zheng Z, Yuan Y, Zhao J, Waclawik ER, Ke X, Zhu H (2009) An efficient photocatalyst structure: TiO_2(B) nanofibers with a shell of anatase nanocrystals. J Am Chem Soc 131: 17885–17893

Yang D, Sarina S, Zhu H, Liu H, Zheng Z, Xie M, Smith SV, Komarneni S (2011) Capture of radioactive cesium and iodide ions from water by using titanate nanofibers and nanotubes. Angew Chem Int Ed 50:10594–10598

Zanini S, Riccardi C, Orlandi M, Fornara V, Colombini M, Donato D, Legnaioli S, Palleschi V (2008) Wood coated with plasma-polymer for water repellence. Wood Sci Technol 42:149–160